
Uncertainty Weighted Actor-Critic for Offline Reinforcement Learning

Yue Wu^{1 2} Shuangfei Zhai¹ Nitish Srivastava¹ Joshua Susskind¹ Jian Zhang¹ Ruslan Salakhutdinov²
Hanlin Goh¹

Abstract

Offline Reinforcement Learning promises to learn effective policies from previously-collected, static datasets without the need for exploration. However, existing Q-learning and actor-critic based off-policy RL algorithms fail when bootstrapping from out-of-distribution (OOD) actions or states. We hypothesize that a key missing ingredient from the existing methods is a proper treatment of uncertainty in the offline setting. We propose Uncertainty Weighted Actor-Critic (UWAC), an algorithm that detects OOD state-action pairs and down-weights their contribution in the training objectives accordingly. Implementation-wise, we adopt a practical and effective dropout-based uncertainty estimation method that introduces very little overhead over existing RL algorithms. Empirically, we observe that UWAC substantially improves model stability during training. In addition, UWAC out-performs existing offline RL methods on a variety of competitive tasks, and achieves significant performance gains over the state-of-the-art baseline on datasets with sparse demonstrations collected from human experts.

1. Introduction

Deep reinforcement learning (RL) has seen a surge of interest over the recent years. It has achieved remarkable success in simulated tasks (Silver et al., 2017; Schulman et al., 2017; Haarnoja et al., 2018), where the cost of data collection is low. However, one of the drawbacks of RL is its difficulty of learning from prior experiences. Therefore, the application of RL to unstructured real-world tasks is still in its primal stages, due to the high cost of active data collection. It is thus crucial to make full use of previously collected datasets whenever large scale online RL is infeasible.

Offline batch RL algorithms offer a promising direction to

¹Apple Inc. ²Carnegie Mellon University. Correspondence to: Yue Wu <ywu5@andrew.cmu.edu>.

leveraging prior experience (Lange et al., 2012). However, most prior off-policy RL algorithms (Haarnoja et al., 2018; Munos et al., 2016; Kalashnikov et al., 2018; Espenholt et al., 2018; Peng et al., 2019) fail on offline datasets, even on expert demonstrations (Fu et al., 2020). The sensitivity to the training data distribution is a well known issue in practical offline RL algorithms (Fujimoto et al., 2019; Kumar et al., 2019; 2020; Peng et al., 2019; Yu et al., 2020). A large portion of this problem is attributed to actions or states not being covered within the training set distribution. Since the value estimate on out-of-distribution (OOD) actions or states can be arbitrary, OOD value or reward estimates can incur destructive estimation errors that propagates through the Bellman loss and destabilizes training. Prior attempts try to avoid OOD actions or states by imposing strong constraints or penalties that force the actor distribution to stay within the training data (Kumar et al., 2019; 2020; Fujimoto et al., 2019; Laroche et al., 2019). While such approaches achieve some degree of experimental success, they suffer from the loss of generalization ability of the Q function. For example, a state-action pair that does not appear in the training set can still lie within the training set distribution, but policies trained with strong penalties will avoid the unseen states regardless of whether the Q function can produce an accurate estimate of the state-action value. Therefore, strong penalty based solutions often promote a pessimistic and sub-optimal policy. In the extreme case, e.g., in certain benchmarking environments with human demonstrations, the best performing offline algorithms only achieve the same performance as a random agent (Fu et al., 2020), which demonstrates the need of robust offline RL algorithms.

In this paper, we hypothesize that a key aspect of a robust offline RL algorithm is a proper estimation and usage of uncertainty. On the one hand, one should be able to reliably assign an uncertainty score to any state-action pair; on the other hand, there should be a mechanism that utilizes the estimated uncertainty to prevent the model from learning from data points that induce high uncertainty scores.

The first problem relates closely to OOD sample detection, which has been extensively studied in the Bayesian deep learning community. (Gal & Ghahramani, 2016a; Gal, 2016; Osawa et al., 2019), often measured by the uncertainty of the model. We adopt the dropout based approach (Gal &

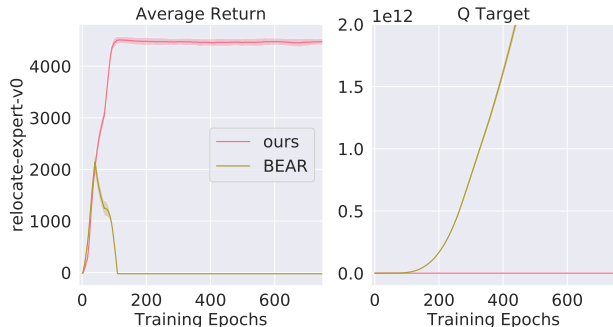


Figure 1: **Left.** Plot of average return v.s. training epochs of our proposed method (red) v.s. baseline (brown) (Kumar et al., 2019) on the relocate-expert offline dataset. **Right.** Corresponding plot of Q-Target values v.s. training epochs. Our proposed method achieves much higher average return, with better training stability, and more controlled Q-values.

Ghahramani, 2016a), due to its simplicity and empirical effectiveness. For the second problem, we provide an intuitive modification to the Bellman updates in actor-critic based algorithms. We then propose Uncertainty Weighted Actor Critic (UWAC), which simply down weights the contribution of target state and action pairs with high uncertainty. By doing so, we prevent the Q function from learning from overly optimistic targets that lie far away from training data distribution (high uncertainty).

Empirically, we first verified the effectiveness of dropout uncertainty estimation at detecting OOD samples. We show that the uncertainty estimation makes intuitive sense in a simple environment. With the uncertainty based down weighting scheme, our method significantly improves the training stability over our chosen baseline (Kumar et al., 2019), and achieves state-of-the-art performance in a variety of standard benchmarking tasks for offline RL.

Overall, our contribution can be summarized as follows: 1) We propose a simple and efficient technique (UWAC) to counter the effect of OOD samples with no additional loss terms or models. 2) We experimentally demonstrate the effectiveness of dropout uncertainty estimation for RL. 3) UWAC offers a novel way for stabilizing offline RL. 4) UWAC achieves SOTA performance on common offline RL benchmarks, and obtains significant performance gain on narrow human demonstrations.

2. Related Work

In this work, we consider offline batch reinforcement learning (RL) under static datasets. Offline RL algorithms are especially prone to errors from inadequate coverage of the training set distribution, distributional shifts during actor critic training, and the variance induced by deep neural networks. Such error have been extensively studied as "error propagation" in approximate dynamic programming

(ADP) (Bertsekas & Tsitsiklis, 1996; Farahmand et al., 2010; Munos, 2003; Scherrer et al., 2015). Scherrer et al. (2015) obtains a bound on the point-wise Bellman error of approximate modified policy iteration (AMPI) with respect to the supremum of the error in function approximation for an arbitrary iteration. We adopt the theoretical tools from (Kumar et al., 2019) and study the accumulation and propagation of Bellman errors under the offline setting.

One of the most significant problems associated with off-policy and offline RL is the bootstrapping error (Kumar et al., 2019): When training encounters an action or state unseen within the training set, the critic value estimate on out-of-distribution (OOD) samples can be arbitrary and incur an error that destabilizes convergence on all other states (Kumar et al., 2019; Fujimoto et al., 2019) through the Bellman backup. Yu et al. (2020) trains a model of the environment that captures the uncertainty. The uncertainty estimate is used to penalize reward estimation for uncertain states and actions, promoting a pessimistic policy against OOD actions and states. The main drawback of such a model based approach is the unnecessary introduction of a model of the environment – it is often very hard to train a good model. On the other hand, model-free approaches either train an agent pessimistic to OOD states and actions (Wu et al., 2019; Kumar et al., 2020) or constrain the actor distribution to the training set action distribution (Fujimoto et al., 2019; Kumar et al., 2019; Wu et al., 2019; Jaques et al., 2019; Fox et al., 2015; Larocche et al., 2019). However, the pessimistic assumption that all unseen states or actions are bad may lead to a sub-optimal agent and greatly reduce generalization to online fine-tuning (Nair et al., 2020). Distributional constraints, in addition, rely on approximations since the actor distribution is often implicit. Such approximations cause practical training instability that we will study in detail in section 5.4.

We propose a model-free actor-critic method that down-weights the Bellman loss term by inverse uncertainty of the critic target. Uncertainty estimation has been implemented in model-free RL for safety and risk estimation (Clements et al., 2019; Hoel et al., 2020) or exploration (Gal & Ghahramani, 2016a; Lines & Van Der Wilk), through ensembling (Hoel et al., 2020) or distributional RL (Dabney et al., 2018; Clements et al., 2019). However, distributional RL works best on discrete action spaces (Dabney et al., 2018) and require additional distributional assumptions when extended to continuous action spaces (Clements et al., 2019). Our approach estimates uncertainty through Monte Carlo dropout (MC-dropout) (Srivastava et al., 2014). MC-dropout uncertainty estimation is a simple method with minimal overhead and has been thoroughly studied in many traditional supervised learning tasks in deep learning (Gal & Ghahramani, 2016a; Hron et al., 2018; Kingma et al., 2015; Gal & Ghahramani, 2016b). Moreover, we observe experimentally

that MC-dropout uncertainty estimation behaves similarly to explicit ensemble models where the prediction is the mean of the ensembles, while being much simpler (Lakshminarayanan et al., 2017; Srivastava et al., 2014).

The most relevant to our work are MOREL (Kidambi et al., 2020), MOPO (Yu et al., 2020), BEAR (Kumar et al., 2019), and CQL (Kumar et al., 2020). MOREL and MOPO approach offline RL from a different model-based paradigm, and obtain competitive results on some tasks with wide data distribution. However, given the model-based nature, MOREL and MOPO achieve limited performance on most other benchmarks due to the performance of the model being limited by the data distribution. On the other hand, BEAR and CQL both use actor-critic and do not suffer from the above problem. We use BEAR (discussed in section 3.2) as our baseline algorithm and achieve significant performance gain through dropout uncertainty weighted backups. CQL avoids OOD states/actions through direct Q value penalty on actions that leads to OOD unseen states within the training set. However the penalty proposed by CQL 1) risks hurting Q estimates for (action, state) pairs that are not OOD, since samples not seen within the dataset can still lie within the true dataset distribution; 2) limits the policy to be pessimistic, which may be hard to fine-tune once on-policy data becomes available. Additionally our method is not limited to BEAR and can apply to other actor-critic methods like CQL. We leave such exploration to future works.

3. Preliminaries

3.1. Notations

Following Kumar et al. (2019), we represent the environment as a Markov decision process (MDP) comprising of a 6-tuple $(\mathcal{S}, \mathcal{A}, P, R, \rho_0, \gamma)$, where \mathcal{S} is the state space, \mathcal{A} is the action space, $P(s'|s, a)$ is the transition probability distribution, ρ_0 is the initial state distribution, $R : \mathcal{S} \times \mathcal{A} \rightarrow \mathbb{R}$ is the reward function, and $\gamma \in (0, 1]$ is the discount factor. Our goal is to find a policy $\pi(s|a)$ from the set of policy functions Π to maximize the expected cumulative discounted reward.

Standard Q-learning learns an optimal state-action value function $Q^*(s, a)$, representing the expected cumulative discounted reward starting from s with action a and then acting optimally thereafter. Q-learning is trained on the Bellman equation defined as follows with the Bellman optimal operator \mathcal{T} defined by:

$$\mathcal{T}Q(s, a) := R(s, a) + \gamma \mathbb{E}_{P(s'|s, a)} \left[\max_{a'} Q(s', a') \right] \quad (1)$$

In practice, the critic (Q function) is updated through dynamic programming, by projecting the target Q estimate ($\mathcal{T}Q$) into Q (i.e. minimizing Bellman Squared Error $\mathbb{E}[(Q - \mathcal{T}Q)^2]$). Since $\max_{a'} Q(s', a')$ in generally in-

tractable in continuous action spaces, an actor (π_θ) function is learned to maximize the critic function ($\pi_\theta(s) := \arg \max_a Q(s, a)$) (Haarnoja et al., 2018; Fujimoto et al., 2018; Sutton & Barto, 2018).

In the context of offline reinforcement learning, naively performing $\max_{a'} Q(s', a')$ in equation 1 may result in an a' unseen within the training dataset (OOD), and resulting in a Q estimate with very large error that can propagate through the Bellman bootstrapping and destabilize training on other states (Kumar et al., 2019).

3.2. Baseline Algorithm

We use BEAR (Kumar et al., 2019) as our baseline algorithm. BEAR restricts the set of policy functions (Π^ϵ) to output actions that lies in the support of the training distribution:

$$\pi(\cdot|s) := \arg \max_{\pi' \in \Pi^\epsilon} \mathbb{E}_{a \sim \pi'(\cdot|s)} [Q(s, a)] \quad (2)$$

Since the true support of $\pi \in \Pi^\epsilon$ is intractable. Kumar et al. (2019) instead relies on an approximate support constraint through optimizing sampled maximum mean discrepancy (MMD) (Gretton et al., 2012) between the training action distribution and the policy distribution.

However, this constraint eliminates the possibility of the Q function to learn to generalize to state-action pairs beyond the training dataset and therefore limits the agent’s performance and generalization. Moreover, the justification behind the sampled MMD approximation as support constraints is largely based on empirical evidence, and we observe numeric instability caused by discrepancies between Q estimates and average returns on some narrower offline datasets (Figure 1). Such observations also correspond to Kumar et al. (2019)’s description in section 7.

4. Uncertainty weighted offline RL

Our approach (UWAC) is motivated by connecting offline RL with the well-established Bayesian uncertainty estimation methods. This connection enables UWAC to “identify” and “ignore” OOD training samples, with no additional models or constraints.

The design choice to use Monte Carlo (MC) dropout for uncertainty estimation is out of implementation simplicity. MC dropout on the Q function has been studied and applied to online RL to encourage exploration through Thompson Sampling (Gal & Ghahramani, 2016a). Despite their limitations as noted by Osband et al. (2018), random prior based methods including dropout have been widely applied to capture uncertainty in RL (Gal & Ghahramani, 2016a; Osband et al., 2018; Fortunato et al., 2017; Lipton et al., 2018; Tang & Kucukelbir, 2017; Touati et al., 2020).

Additionally, we note that uncertainty estimation methods that enforce time-wise or trajectory-wise consistency (Osband et al., 2016; 2018) are incompatible with the offline RL problem since the offline dataset does not necessarily need to contain full trajectories. Our experiments (section 5.1) empirically demonstrate that dropout uncertainty estimation can identify OOD states.

4.1. Uncertainty estimation through dropout

Let X capture all the state-action pairs in the training set: $X = (s, a)$, and Y capture the true Q value of the states. We draw inspiration from a Bayesian formulation for the Q function in RL parameterized by θ , and maximize $p(\theta|X, Y) = p(Y|X, \theta)p(\theta)/p(Y|X)$ as our objective. Since $p(Y|X)$ is generally intractable, we approximate the inference process through dropout variational inference (Gal & Ghahramani, 2016a), by training with dropout before every weight layer, and also performing dropout at test time (referred to as Monte Carlo dropout). The model uncertainty is captured by the approximate predictive variance with respect to the estimated \hat{Q} for T stochastic forward passes

$$\begin{aligned} \text{Var}[Q(s, a)] &\approx \\ \sigma^2 + \frac{1}{T} \sum_{t=1}^T \hat{Q}_t(s, a)^\top \hat{Q}_t(s, a) - E[\hat{Q}(s, a)]^\top E[\hat{Q}(s, a)] \end{aligned}$$

with σ^2 corresponding to the inherent noise in the data, the **second** term corresponding to how much the model is uncertain about its predictions, and $E[\hat{Q}(s, a)]$ the predictive mean. We therefore use the **second**–**third** term to capture model uncertainty for OOD sample detection.

Overall, instead of training a Q^π function and policy π , we define an uncertainty-weighted policy distribution π' with respect to the original policy distribution $\pi(\cdot|s)$, the $Q_0^{\pi'}$ from last training iteration, and normalization factor $Z(s)$

$$\begin{aligned} \pi'(a|s) &= \frac{\beta}{\text{Var}[Q_0^{\pi'}(s, a)]} \pi(a|s)/Z(s); \\ Z(s) &= \int_a \frac{\beta}{\text{Var}[Q_0^{\pi'}(s, a)]} \pi(a|s) da \end{aligned} \quad (3)$$

We show in the appendix A.1 that optimizing π' results in theoretically better convergence properties against OOD training samples.

4.2. Uncertainty Weighted Actor-Critic

Instead of training the Q function on Equation 1, we train Q_θ on π' . For clarity, we denote the TD Q -target as in

(Mnih et al., 2013; Kumar et al., 2019) by $Q_{\theta'}$.

$$\begin{aligned} \mathcal{L}(Q_\theta) &= \mathbb{E}_{(s'|s, a) \sim \mathcal{D}} \mathbb{E}_{a' \sim \pi'(\cdot|s')} [Errr(s, a, s', a')^2] \\ &= \mathbb{E}_{(s'|s, a) \sim \mathcal{D}} \mathbb{E}_{a' \sim \pi(\cdot|s')} \left[\frac{\beta}{\text{Var}[Q_{\theta'}(s', a')]} Errr(s, a, s', a')^2 \right] \\ Errr(s, a, s', a') &= Q_\theta(s, a) - (R(s, a) + \gamma Q_{\theta'}(s', a')). \end{aligned} \quad (4)$$

We absorb the normalization factor Z into β . The resulting training loss down-weights the Bellman loss for the Q function by inverse the uncertainty of the Q -target ($Q_{\theta'}(s', a')$) that does track gradient. This directly reduces the effect that OOD backups has on the overall training process.

Similarly, we optimize the actor π using samples from π' . Substituting $\pi(\cdot|s)$ by $\pi'(\cdot|s)$ in equation 2, we arrive at the following actor loss

$$\begin{aligned} \mathcal{L}(\pi) &= -\mathbb{E}_{a \sim \pi'(\cdot|s)} [Q_\theta(s, a)] \\ &= -\mathbb{E}_{a \sim \pi(\cdot|s)} \left[\frac{\beta}{\text{Var}[Q_\theta(s, a)]} Q_\theta(s, a) \right] \end{aligned} \quad (5)$$

The resulting actor loss intuitively decreases the probability of maximizing the Q function on OOD samples, further discouraging the vicious cycle of Q function explosion. Such loss further stabilizes Q function estimations without constraints on the actor function distribution.

Algorithm 1 summarizes the proposed training curriculum, mostly the same as in the baseline (Kumar et al., 2019). Note that we do not propagate gradient through the uncertainty ($\text{Var}(y(s, a))$)

5. Experimental Results

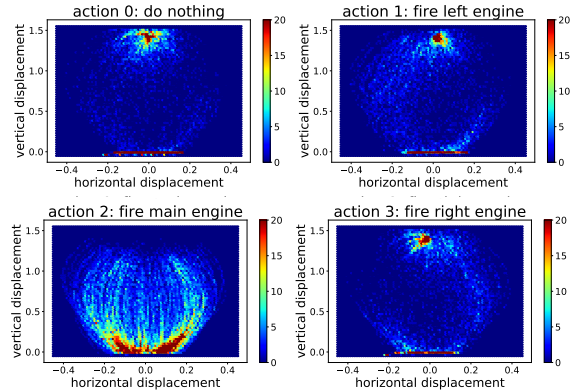


Figure 2: **Expert Trajectory Visualization.** 2D heat maps of the expert’s action distribution with respect to horizontal/vertical displacement from the goal location. Warmer locations represent more observations.

Our experiments are structured as follows: In section 5.1, we validate and visualize the effectiveness of dropout uncertainty estimation in RL. In section 5.2 we present competitive benchmarking results on the widely-used D4RL MuJoCo walkers dataset. We then experiment with the more

Algorithm 1 Pseudo code for UWAC, differences from (Kumar et al., 2019) are colored

- Input:** Dataset \mathcal{D} , target network update rate τ , mini-batch size N , sampled actions for MMD ($n = 10$), **sample numbers stochastic forward passes** ($T = 100$), hyperparameters: λ, α, β
- 1: Initialize Q networks $\{Q_{\theta_1}, Q_{\theta_2}\}$ with **MC Dropout**. Initialize actor π_{ϕ} , target networks $\{Q_{\theta'_1}, Q_{\theta'_2}\}$ and a target actor $\pi_{\phi'}$, with $\phi' \leftarrow \phi, \theta'_{1,2} \leftarrow \theta_{1,2}$
 - 2: **for** $t \leftarrow 1$ to N **do**
 - 3: Sample mini-batch of transitions $(s, a, r, s') \sim \mathcal{D}$
 - 4: **Q-update:**
 - 5: Sample p action samples, $\{a_i \sim \pi_{\phi'}(\cdot|s')\}_{i=1}^p$
 - 6: $y(s, a) := \max_{a_i} [\lambda \min(Q_{\theta'_1}(s', a_i), Q_{\theta'_2}(s', a_i)) + (1 - \lambda) \max(Q_{\theta'_1}(s', a_i), Q_{\theta'_2}(s', a_i))]$
 - 7: **Calculate variance of the $y(s, a)$ through variance of T stochastic samples from $Q_{\theta'_1}, Q_{\theta'_2}$**
 - 8: Perform one step of SGD to minimize $\mathcal{L}(Q_{\theta_{1,2}}) = \frac{\beta}{\text{Var}[y(s, a)]} (Q_{\theta_{1,2}}(s, a) - (r + \gamma y(s, a)))^2$
 - 9: **Policy-update:**
 - 10: Sample actions $\{a_i \sim \pi_{\phi'}(\cdot|s')\}_{i=1}^m, \{a_j \sim \mathcal{D}\}_{i=1}^n$
 - 11: Update ϕ, a according to **equation 5** with MMD penalty with weight α as in section 3.2
 - 12: **Update Target Networks:** $\theta'_{1,2} \leftarrow \tau \theta_{1,2}; \phi'_i \leftarrow \tau \phi_i$
 - 13: **end for**

complex Adroit hand manipulation environment in section 5.3, and analyze the training stability and the effectiveness against OOD samples by examining the Q target functions in section 5.4. We report the implementation details in section 5.5, ablation studies 5.6, and training time in A.2.

5.1. Dropout Uncertainty Estimation for Reinforcement Learning

For the ease of 2D-visualization, we firstly investigate the effectiveness of MC dropout for uncertainty estimation on the OpenAI gym LunarLander-v2 environment. The LunarLander-v2 environment features a lunar lander agent trying to land at a goal location in a 2D world (between two yellow flags) with 4 actions {do nothing, fire left engine, fire downward engine, fire right engine}.

We generate the expert offline dataset from the final replay buffer (size 100,000) of a fully trained expert AWR (Peng et al., 2019) agent with average reward 270. Note that the state-action distribution has a relatively complete coverage over the observation space (Fig. 2).

To simulate the scenario in most offline datasets, where the agent encounters lots of out-of-distribution states and actions, we create two skewed datasets by removing all observations from the upper-half or the leftmost-half according to displacement from objective. We visualize the

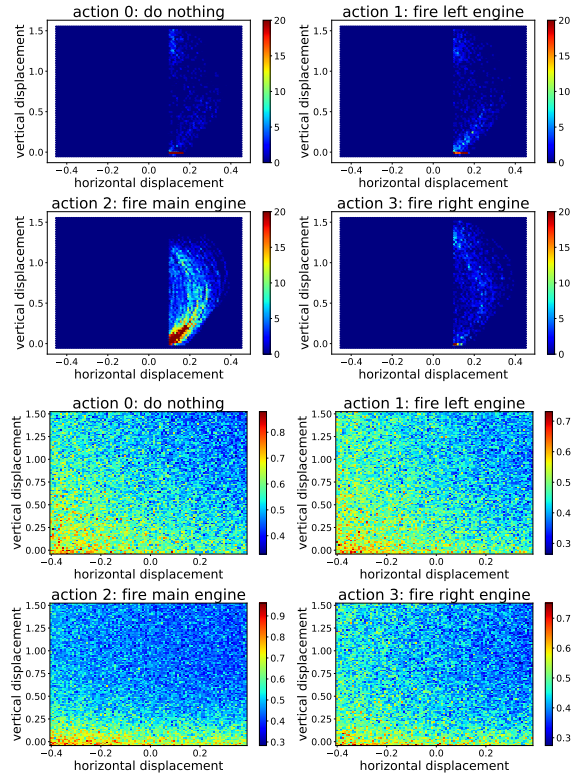


Figure 3: **Top.** The training set with horizontal displacements (< 0.1) removed. This makes all states on the left OOD. **Bottom.** Our model estimates higher uncertainty (brighter color) on the left and lower uncertainty (colder color) on the right.

We visualize the heatmap with the average speed of the lander, which is faster than observations at the bottom of the map. As a result, Fig 2 does not represent the actual frequency of training data, and the uncertainty should be compared horizontally, not vertically.

clipped datasets distribution together with the estimated Q function uncertainty in Figure 3,7. Our proposed framework reports higher uncertainty estimates at locations where the observations are sparse, especially where the observations are removed (OOD states). The results demonstrate the effectiveness of our proposed method at estimating the uncertainty of the Q function.

Additionally, in some benchmarking experiments, we observe lower uncertainty estimates of state-action pairs in the training set than states from the training set paired with random actions (as in Figure 4 for the walker2d-expert task). This further validates the use of MC dropout as a way to detect OOD state-action pairs.

5.2. Performance on standard benchmarking datasets for offline RL

We evaluate our method on the MuJoCo datasets in the D4RL benchmarks (Fu et al., 2020), including three environments (halfcheetah, hopper, and walker2d) and five dataset types (random, medium, medium-replay, medium-expert,



Figure 4: Uncertainty (estimated as variance) of state-action pairs from the (walker2d-expert) training dataset (green) compared to uncertainty estimates of the states combined with random actions from the same dataset.

Since the action space for robotic control is quite small and noisy, a lot of random actions are actually in-distribution. Although the regions overlap, we achieve a ROC/AUC score of 0.845 for identifying OOD actions.

expert), yielding a total of 15 problem settings. The datasets in this benchmark have been generated as follows: **random**: roll out a randomly initialized policy for 1M steps. **expert**: 1M samples from a policy trained to completion with SAC. **medium**: 1M samples from a policy trained to approximately 1/3 the performance of the expert. **medium-replay**: replay buffer of a policy trained up to the performance of the medium agent. **medium-expert**: 50-50 split of medium and expert data.

Results are shown in Table 1. Our method is the strongest by a significant margin on all the medium-expert datasets and most of the medium-expert datasets, and also achieves good performance on all of the random and medium datasets, where the datasets lack state/action diversity. Our approach performs less well on the medium-replay datasets compared to model based method (MOPO) because model-based methods typically perform well on datasets with diverse state/action.

5.3. Performance on Adroit hand dataset with human demonstrations

We then experiment with a more complex robotic hand manipulation dataset. The Adroit dataset in the D4RL benchmarks (Rajeswaran et al., 2017) involves controlling a 24-DoF simulated hand to perform 4 tasks including hammering a nail, opening a door, twirling a pen, and picking/moving a ball. This dataset is particularly hard for previous state-of-the-art works in that it contains of narrow human demonstrations on a high-dimensional robotic

manipulation task.



Figure 5: Our learned policies successfully accomplishes manipulation tasks, such as opening a door as shown.

The dataset contains three types of datasets for each task. **human**: a small amount of demonstration data from a human; **expert**: a large amount of expert data from a fine-tuned RL policy; **cloned**: the third dataset is generated by imitating the human data, running the policy, and mixing data at a 50-50 ratio with the demonstrations. It is worth noting that mixing (for cloned) is performed because the cloned policies themselves do not successfully complete the task, making the dataset otherwise difficult to learn from (Fu et al., 2020).

Results are shown in Table 2. UWAC achieves significant improvement on the baseline (BEAR) (Kumar et al., 2019) on all the “human” demonstration datasets, where the datasets lacks state/action diversity and the agent will encounter lots of OOD backups during training. We also obtain state-of-the art performance all other datasets in Adroit.

5.4. Analysis of Training Dynamics

Although the baseline method BEAR (Kumar et al., 2019) already improves offline RL training stability on most of the MuJoCo Walkers dataset, we observe significantly worse training stability when training BEAR on the more complex Adroit hand dataset, especially on demonstrations collected from a narrow policy (i.e. human demonstrations). We show some selected results in Figure 6.

Note that on 5 of the 6 panels shown, the performance of BEAR drops after obtaining peak very early on into training, and sometimes even falls back to initial performance. We also observe similar behavior in all other environments, see full adroit results in Figure 8 in the Appendix. Additionally, we observe strong correlation between the training instability and the explosion of Q values. All performance drops begin at within 5 epochs when Q target estimate greatly exceeds the average return. We attribute the problem of Q function over-estimation and explosion to performing backups from OOD states and actions: As performance improves initially, the OOD Q estimates increases together with the average Q estimates. Since the agent is unable to explore on the OOD actions/states, any over-estimation on the OOD samples can further increase average Q estimates through the Bellman backups, causing a vicious cycle leading to Q value explosion.

In the initial stages of training, the performance of UWAC increases together with the baseline. By down-weighting the OOD backups, UWAC breaks the vicious cycle, and maintains meaningful Q estimates throughout training. This

Table 1: Normalized Average Returns of UWAC v.s. previous state-of-the-arts (BEAR, CQL, MOPO) and random ensemble mixtures (REM), and AlgaeDICE (aDICE) on the D4RL MuJoCo Gym dataset according to (Fu et al., 2020). We report the average over 5 random seeds (\pm standard deviation). BEAR, CQL do not report standard deviation. We omit BRAC-p and SAC-off because they do not obtain performance meaningful for comparison. We **bold** the highest mean.

Task Name	UWAC (OURS)	MOPO	MOReL	BEAR	BRACv	AWR	BCQ	BC	CQL	REM	aDICE
halfcheetah-random	14.5 \pm 3.3	35.4 \pm 2.5	25.6	25.1	31.2	2.5	2.2	2.1	35.4	-2.6	-0.3
walker2d-random	15.5 \pm 11.7	13.6 \pm 2.6	37.3	7.3	1.9	1.5	4.9	1.6	7	-0.3	0.5
hopper-random	22.4 \pm 12.1	11.7 \pm 0.4	53.6	11.4	12.2	10.2	10.6	9.8	10.8	0.7	0.9
halfcheetah-medium	46.5 \pm 2.5	42.3 \pm 1.6	42.1	41.7	46.3	37.4	40.7	36.1	44.4	-2.6	-2.2
walker2d-medium	57.5 \pm 7.8	17.8 \pm 19.3	77.8	59.1	81.1	17.4	53.1	6.6	79.2	-0.2	0.3
hopper-medium	88.9 \pm 12.2	28.0 \pm 12.4	95.4	52.1	31.1	35.9	54.5	29.0	58	0.6	1.2
halfcheetah-med-replay	46.8 \pm 3.0	53.1 \pm 2.0	40.2	38.6	47.7	40.3	38.2	38.4	46.2	-3.0	-2.1
walker2d-med-replay	27.0 \pm 6.3	39.0 \pm 9.6	49.8	19.2	0.9	15.5	15.0	11.3	26.7	-0.2	0.6
hopper-med-replay	39.4 \pm 6.1	67.5 \pm 24.7	93.6	33.7	0.6	28.4	33.1	11.8	48.6	0.8	1.1
halfcheetah-med-expert	127.4 \pm 3.7	63.3 \pm 38.0	53.3	53.4	41.9	52.7	64.7	35.8	62.4	-2.6	-0.8
walker2d-med-expert	99.7 \pm 12.2	44.6 \pm 12.9	95.6	40.1	81.6	53.8	57.5	6.4	98.7	-0.2	0.4
hopper-med-expert	134.7 \pm 21.2	23.7 \pm 6.0	108.7	96.3	0.8	27.1	110.9	111.9	111	0.7	1.1
halfcheetah-expert	128.6 \pm 2.9	-	-	108.2	-1.1	-	-	107	104.8	-	-
walker2d-expert	121.1 \pm 22.4	-	-	106.1	0	-	-	125.7	153.9	-	-
hopper-expert	135.0 \pm 14.1	-	-	110.3	3.7	-	-	109	109.9	-	-

Table 2: Normalized Average Returns on the D4RL Adroit dataset in the same format as Table 1, over 5 random seeds (\pm standard deviation). We omit BRAC-p, BRAC-v because they do not obtain performance meaningful for comparison.

Task Name	UWAC (OURS)	BEAR	BC	SAC-off	CQL(\mathcal{H})	CQL(ρ)	AWR	BCQ	SAC-on	REM	aDICE
pen-human	65.0 \pm 3.0	-1.0	34.4	6.3	37.5	55.8	12.3	68.9	21.6	3.5	-3.3
hammer-human	8.3 \pm 7.9	0.3	1.5	0.5	4.4	2.1	1.2	0.5	0.2	0.2	0.3
door-human	10.7 \pm 5.5	-0.3	0.5	3.9	9.9	9.1	0.4	0.0	-0.2	-0.1	-0.0
relocate-human	0.5 \pm 0.6	-0.3	0.0	0.0	0.2	0.4	0.0	-0.1	-0.2	-0.2	-0.1
pen-cloned	45.1 \pm 5.8	26.5	56.9	23.5	39.2	40.3	28.0	44.0	21.6	-3.4	-2.9
hammer-cloned	1.2 \pm 3.4	0.3	0.8	0.2	2.1	5.7	0.4	0.4	0.2	0.2	0.3
door-cloned	1.2 \pm 3.6	-0.1	-0.1	0.0	0.4	3.5	0.0	0.0	-0.2	-0.1	0.0
relocate-cloned	0.0 \pm 0.2	-0.3	-0.1	-0.2	-0.1	-0.1	-0.2	-0.3	-0.2	-0.2	-0.3
pen-expert	119.8 \pm 4.1	105.9	85.1	6.1	-	-	111.0	114.9	21.6	0.3	-3.5
hammer-expert	128.8 \pm 4.8	127.3	125.6	25.2	-	-	39.0	107.2	0.2	0.2	0.3
door-expert	105.4 \pm 2.1	103.4	34.9	7.5	-	-	102.9	99.0	-0.2	-0.2	0.0
relocate-expert	108.7 \pm 1.7	98.6	101.3	-0.3	-	-	91.5	41.6	-0.2	-0.1	-0.1

allows UWAC to further train on the offline dataset and surpass BEAR after the performance drop and maintain positive performance.

5.5. Implementation Details

LunarLander: We set our expert to be a simple 3-layer actor-critic agent trained to completion with (Peng et al., 2019). We take the final replay buffer (size 100,000) with average reward of 269.7. The vertically clipped dataset in Figure 7 contains 76,112 samples, and the horizontally clipped dataset in Figure 3 contains 21,038 samples.

We then train a simple 3-layer actor-critic off-policy agent on the clipped datasets according to Algorithm 1 (we do not take the MMD loss in line 11 to enlarge the effect of OOD samples).

Baseline (BEAR): We ran benchmarks on the official

GitHub code¹ of BEAR and the updated version² provided by the authors. We ran parameter search on all the recommended parameters `kernel_type` \in {gaussian, laplacian}, `mmd_sigma` \in {10,20}, 100 actions sampled for evaluation, and 0.07 being the `mmd_target_threshold`. We are able to reproduce the results reported in (Fu et al., 2020) with both the official GitHub and the updated version.

Our method (UWAC): We apply our weighted loss to Algorithm 1 to the updated BEAR code provided by Kumar et al. (2019). We keep the hyper-parameters and the network architecture exactly the same as in BEAR. For experiments on the Adroit hand environment, we further enforce Spectral Norm on the Q function for better stability similar to (Yu et al., 2020) and theoretical guarantee as shown in Appendix A.1. We clip the inverse variance to within the range of (0.0, 1.5) for numerical stability.

¹github.com/aviralkumar2907/BEAR

²github.com/rail-berkeley/d4rl_evaluations

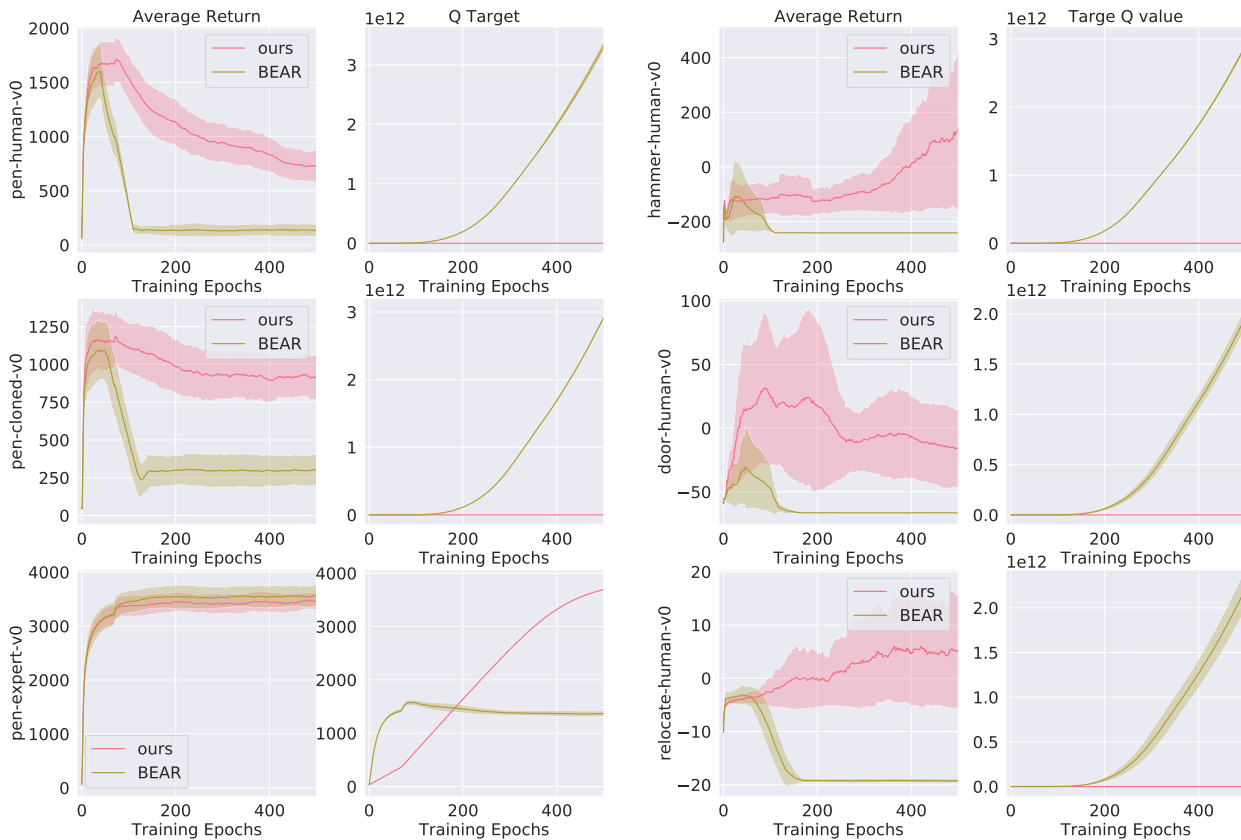


Figure 6: Plot of average return v.s. training epochs, together with the corresponding average Q Target over training epochs. Results are averaged across 5 random seeds. **Left:** Results of different types (human, cloned, expert) on the Adroit pen task. **Right:** Results on human demos on the 3 remaining tasks. The performance of baseline (BEAR) degrades over time (also noted in (Kumar et al., 2019)), and the Target Q value explodes.

For the choice of β in Algorithm 1, we swept over values from the set $\{0.8, 1.6, 2.5\}$, determined by matching the average uncertainty output during training time. We found that the model is quite robust against β : 0.8, 1.6 gave similarly good performance across all tasks in our experiments. We also note that β can be absorbed into the learning rate since it acts both on the actor loss and critic loss. However, since the MMD loss from BEAR is not β -weighted, we make the design choice to tune β in stead of the MMD weight α .

5.6. Ablations

Spectral Normalization: Our first study isolates the effect of Spectral Norm on the performance. Although BEAR + Spectral Norm enforces a bounded Q function and maintains good training stability, Spectral Norm does not handle OOD backups on the narrow Adroit datasets. We discover experimentally that BEAR+SN performs much worse than BEAR only, we plot the complete results of BEAR+SN v.s. BEAR in Figure 10.

Dropout/Ensembles for Regularization: Our second study isolates the effect of Dropout on the performance as a regularizer, since dropout alone does not handle OOD

backups on the narrow Adroit datasets. We observe experimentally that UWAC without uncertainty weighing (BEAR+Dropout+Spectral Norm) does not change the behavior of BEAR under Spectral Norm (Figure 11) and performs worse than UWAC (Figure 12) and the original BEAR (Figure 13). In addition, we note that ensemble based methods like REM (Agarwal et al., 2020) alone achieves bad performance on the Adroit environment (Table 1,2).

Replacing Dropout with Ensembles: To verify the generalization of UWAC to uncertainty estimation methods beyond dropout, we applied UWAC loss to ensembles trained under REM (Agarwal et al., 2020) and average-DQN ensembles (Anschel et al., 2017). In both cases, UWAC still outperforms baseline (BEAR). We notice that dropout has very similar performance as average-DQN ensembles on the Adroit dataset (Figure 14).

Down-weight by Variance v.s. Standard Deviation: We notice no significant difference in behavior down-weighting using standard deviation or variance (Figure 15).

6. Conclusion and Future Work

In this work, we have leveraged uncertainty estimation to detect and down-weight OOD backups in the Bellman squared loss for offline RL. We show our proposed technique, UWAC, achieves superior performance and improved training stability, without introducing any additional model or losses. Furthermore, we experimentally demonstrate the effectiveness of dropout uncertainty estimation at detecting OOD samples in offline RL. UWAC also can be applied to stabilize other actor-critic methods, and we leave the investigation to future works.

In addition, our work demonstrates a valuable application of uncertainty estimation in RL. Future works can combine model-based and model-free methods for offline or off-policy RL and use uncertainty estimation to decide when to use the model to train the actor. Additionally, uncertainty estimation may be used to guide curiosity based RL agents for on-policy curiosity-based learning.

References

- Agarwal, R., Schuurmans, D., and Norouzi, M. An optimistic perspective on offline reinforcement learning. In *International Conference on Machine Learning*, pp. 104–114. PMLR, 2020.
- Anschel, O., Baram, N., and Shimkin, N. Averaged-dqn: Variance reduction and stabilization for deep reinforcement learning. In *International Conference on Machine Learning*, pp. 176–185. PMLR, 2017.
- Bertsekas, D. P. and Tsitsiklis, J. N. *Neuro-dynamic programming*. Athena Scientific, 1996.
- Clements, W. R., Robaglia, B.-M., Van Delft, B., Slaoui, R. B., and Toth, S. Estimating risk and uncertainty in deep reinforcement learning. *arXiv preprint arXiv:1905.09638*, 2019.
- Dabney, W., Rowland, M., Bellemare, M. G., and Munos, R. Distributional reinforcement learning with quantile regression. In *AAAI*, 2018.
- Espeholt, L., Soyer, H., Munos, R., Simonyan, K., Mnih, V., Ward, T., Doron, Y., Firoiu, V., Harley, T., Dunning, I., et al. Impala: Scalable distributed deep-rl with importance weighted actor-learner architectures. In *ICML*, 2018.
- Farahmand, A.-m., Szepesvári, C., and Munos, R. Error propagation for approximate policy and value iteration. In *Advances in Neural Information Processing Systems*, pp. 568–576, 2010.
- Fortunato, M., Azar, M. G., Piot, B., Menick, J., Osband, I., Graves, A., Mnih, V., Munos, R., Hassabis, D., Pietquin, O., et al. Noisy networks for exploration. *arXiv preprint arXiv:1706.10295*, 2017.
- Fox, R., Pakman, A., and Tishby, N. Taming the noise in reinforcement learning via soft updates. *arXiv preprint arXiv:1512.08562*, 2015.
- Fu, J., Kumar, A., Nachum, O., Tucker, G., and Levine, S. D4rl: Datasets for deep data-driven reinforcement learning. *arXiv preprint arXiv:2004.07219*, 2020.
- Fujimoto, S., van Hoof, H., Meger, D., et al. Addressing function approximation error in actor-critic methods. *Proceedings of Machine Learning Research*, 80, 2018.
- Fujimoto, S., Meger, D., and Precup, D. Off-policy deep reinforcement learning without exploration. In *International Conference on Machine Learning*, pp. 2052–2062, 2019.
- Gal, Y. Uncertainty in deep learning. *University of Cambridge*, 1(3), 2016.
- Gal, Y. and Ghahramani, Z. Dropout as a bayesian approximation: Representing model uncertainty in deep learning. In *international conference on machine learning*, pp. 1050–1059, 2016a.
- Gal, Y. and Ghahramani, Z. A theoretically grounded application of dropout in recurrent neural networks. In *Advances in neural information processing systems*, pp. 1019–1027, 2016b.
- Gretton, A., Borgwardt, K. M., Rasch, M. J., Schölkopf, B., and Smola, A. A kernel two-sample test. *The Journal of Machine Learning Research*, 13(1):723–773, 2012.
- Haarnoja, T., Zhou, A., Abbeel, P., and Levine, S. Soft actor-critic: Off-policy maximum entropy deep reinforcement learning with a stochastic actor. In *International Conference on Machine Learning*, pp. 1861–1870, 2018.
- Hoel, C.-J., Tram, T., and Sjöberg, J. Reinforcement learning with uncertainty estimation for tactical decision-making in intersections. *arXiv preprint arXiv:2006.09786*, 2020.
- Hron, J., Matthews, A., and Ghahramani, Z. Variational bayesian dropout: pitfalls and fixes. In *International Conference on Machine Learning*, pp. 2019–2028, 2018.
- Jaques, N., Ghandeharioun, A., Shen, J. H., Ferguson, C., Lapedriza, A., Jones, N., Gu, S., and Picard, R. Way off-policy batch deep reinforcement learning of implicit human preferences in dialog. *arXiv preprint arXiv:1907.00456*, 2019.
- Kalashnikov, D., Irpan, A., Pastor, P., Ibarz, J., Herzog, A., Jang, E., Quillen, D., Holly, E., Kalakrishnan, M., Vanhoucke, V., et al. Scalable deep reinforcement learning for vision-based robotic manipulation. In *Conference on Robot Learning*, pp. 651–673, 2018.
- Kidambi, R., Rajeswaran, A., Netrapalli, P., and Joachims, T. Morel: Model-based offline reinforcement learning. *arXiv preprint arXiv:2005.05951*, 2020.
- Kingma, D. P., Salimans, T., and Welling, M. Variational dropout and the local reparameterization trick. In *Advances in neural information processing systems*, pp. 2575–2583, 2015.
- Kumar, A., Fu, J., Soh, M., Tucker, G., and Levine, S. Stabilizing off-policy q-learning via bootstrapping error reduction. In *Advances in Neural Information Processing Systems*, pp. 11784–11794, 2019.
- Kumar, A., Zhou, A., Tucker, G., and Levine, S. Conservative q-learning for offline reinforcement learning. *arXiv preprint arXiv:2006.04779*, 2020.

- Lakshminarayanan, B., Pritzel, A., and Blundell, C. Simple and scalable predictive uncertainty estimation using deep ensembles. In *Advances in neural information processing systems*, pp. 6402–6413, 2017.
- Lange, S., Gabel, T., and Riedmiller, M. Batch reinforcement learning. In *Reinforcement learning*, pp. 45–73. Springer, 2012.
- Laroche, R., Trichelair, P., and Des Combes, R. T. Safe policy improvement with baseline bootstrapping. In *International Conference on Machine Learning*, pp. 3652–3661. PMLR, 2019.
- Lines, D. and Van Der Wilk, M. Disentangling sources of uncertainty for active exploration.
- Lipton, Z., Li, X., Gao, J., Li, L., Ahmed, F., and Deng, L. Bbq-networks: Efficient exploration in deep reinforcement learning for task-oriented dialogue systems. In *Proceedings of the AAAI Conference on Artificial Intelligence*, volume 32, 2018.
- Mnih, V., Kavukcuoglu, K., Silver, D., Graves, A., Antonoglou, I., Wierstra, D., and Riedmiller, M. Playing atari with deep reinforcement learning. *arXiv preprint arXiv:1312.5602*, 2013.
- Munos, R. Error bounds for approximate policy iteration. In *ICML*, volume 3, pp. 560–567, 2003.
- Munos, R., Stepleton, T., Harutyunyan, A., and Bellemare, M. Safe and efficient off-policy reinforcement learning. In *Advances in Neural Information Processing Systems*, pp. 1054–1062, 2016.
- Nair, A., Dalal, M., Gupta, A., and Levine, S. Accelerating online reinforcement learning with offline datasets. *arXiv preprint arXiv:2006.09359*, 2020.
- Osawa, K., Swaroop, S., Khan, M. E. E., Jain, A., Eschenhagen, R., Turner, R. E., and Yokota, R. Practical deep learning with bayesian principles. In *Advances in neural information processing systems*, pp. 4287–4299, 2019.
- Osband, I., Blundell, C., Pritzel, A., and Van Roy, B. Deep exploration via bootstrapped dqn. In *Advances in neural information processing systems*, pp. 4026–4034, 2016.
- Osband, I., Aslanides, J., and Cassirer, A. Randomized prior functions for deep reinforcement learning. In *Advances in Neural Information Processing Systems*, pp. 8617–8629, 2018.
- Peng, X. B., Kumar, A., Zhang, G., and Levine, S. Advantage-weighted regression: Simple and scalable off-policy reinforcement learning. *arXiv preprint arXiv:1910.00177*, 2019.
- Rajeswaran, A., Kumar, V., Gupta, A., Vezzani, G., Schulman, J., Todorov, E., and Levine, S. Learning complex dexterous manipulation with deep reinforcement learning and demonstrations. *arXiv preprint arXiv:1709.10087*, 2017.
- Scherrer, B., Ghavamzadeh, M., Gabillon, V., Lesner, B., and Geist, M. Approximate modified policy iteration and its application to the game of tetris. *J. Mach. Learn. Res.*, 16:1629–1676, 2015.
- Schulman, J., Wolski, F., Dhariwal, P., Radford, A., and Klimov, O. Proximal policy optimization algorithms. *arXiv preprint arXiv:1707.06347*, 2017.
- Silver, D., Schrittwieser, J., Simonyan, K., Antonoglou, I., Huang, A., Guez, A., Hubert, T., Baker, L., Lai, M., Bolton, A., et al. Mastering the game of go without human knowledge. *nature*, 550(7676):354–359, 2017.
- Srivastava, N., Hinton, G., Krizhevsky, A., Sutskever, I., and Salakhutdinov, R. Dropout: a simple way to prevent neural networks from overfitting. *The journal of machine learning research*, 15(1):1929–1958, 2014.
- Sutton, R. S. and Barto, A. G. *Reinforcement learning: An introduction*. MIT press, 2018.
- Tang, Y. and Kucukelbir, A. Variational deep q network. *arXiv preprint arXiv:1711.11225*, 2017.
- Touati, A., Satija, H., Romoff, J., Pineau, J., and Vincent, P. Randomized value functions via multiplicative normalizing flows. In *Uncertainty in Artificial Intelligence*, pp. 422–432. PMLR, 2020.
- Wu, Y., Tucker, G., and Nachum, O. Behavior regularized offline reinforcement learning. *arXiv preprint arXiv:1911.11361*, 2019.
- Yu, T., Thomas, G., Yu, L., Ermon, S., Zou, J., Levine, S., Finn, C., and Ma, T. Mopo: Model-based offline policy optimization. *arXiv preprint arXiv:2005.13239*, 2020.

A. Appendix

A.1. Analysis for Convergence Properties

We first extend the convergence theorem (Theorem B.1) from (Kumar et al., 2019) to obtain a bound on the approximation error with respect to bellman approximation error $\delta(s, a)$ – Theorem A.1.

Note that Theorem A.1 alone does not imply convergence, since $\delta(s, a)$ can be arbitrarily large due to OOD estimates in offline RL. We then show (in Theorem A.2) that $\delta(s, a)$ can be bounded by any constant under mild assumptions that the Q function is Lipschitz continuous. Theorem A.2 shows our framework converges w.r.t. OOD samples.

Theorem A.1. *Suppose we run approximate distribution-constrained value iteration with a set constrained backup \mathcal{T}^Π on a set of policies Π . Let $\delta(s, a)$ be the upper-bound for the Bellman approximation error for a given state-action pair (s, a) over k training steps: $\delta(s, a) = \sup_k |Q_k(s, a) - \mathcal{T}^\Pi Q_{k-1}(s, a)|$. Then,*

$$\begin{aligned} & \lim_{k \rightarrow \infty} \mathbb{E}_{\rho_0} [|V_k(s) - V^*(s)|] \\ & \leq \frac{\gamma}{(1-\gamma)^2} \left[C(\Pi) \mathbb{E}_\mu \left[\max_{\pi \in \Pi} \mathbb{E}_\pi [\delta(s, a)] \right] + \frac{1-\gamma}{\gamma} \alpha(\Pi) \right] \end{aligned}$$

with the suboptimality constant $(\alpha(\Pi))$ and the concentrability coefficient defined as:

$$\begin{aligned} \alpha(\Pi) &= \max_{s,a} |\mathcal{T}^\Pi Q^*(s, a) - \mathcal{T} Q^*(s, a)|; \\ C(\Pi) &\stackrel{\text{def}}{=} (1-\gamma)^2 \sum_{k=1}^{\infty} k \gamma^{k-1} c(k) \end{aligned}$$

The proof of the theorem is a direct modification of the contraction proof in Theorem 3 of (Farahmand et al., 2010) or Theorem 1 of (Munos, 2003).

The *suboptimality constant* $(\alpha(\Pi))$ captures how far π^* is from Π , namely the suboptimality of the actor. The *concentrability coefficient* quantifies how far the visitation distribution generated by policies from Π is from the training data distribution, namely the degree to which the training may encounter OOD actions and states. Kumar et al. (2019) note a trade-off between $\alpha(\Pi)$ and $C(\Pi)$, and propose to bound both terms by constraining Π to the set of policies with support the same as the training set policy with MMD loss.

However, the most important Bellman approximation error term which is the root cause of the bootstrapping problem is still left unbounded. We proceed to show that for $\pi'(a|s) = \frac{\beta}{\sup_k \sqrt{\text{Var}[Q_k(s, a)]}} \pi(a|s)/Z$. Assuming that $Z \geq 1$, and that Q is bounded, we can bound the Bellman error term $\max_{\pi'} \mathbb{E}_{\pi'} [\delta(s, a)]$ by any constant C with arbitrarily high probability by optimizing on π' .

Note that Theorem A.2 considers down-weighting by inverse the square-root of the variance (standard deviation), which is different from the inverse variance in Equation 3,4,5 and Algorithm 1. Down-weighting by the variance has the same practical effect since we clip the ratio for numerical stability. We adopt variance for practical implementation for the ease of tracing after multiple max,min,summation operations in Algorithm 1.

Theorem A.2. *Let $\pi'(a|s) = \frac{\beta}{\sup_k \sqrt{\text{Var}[Q_k(s, a)]}} \pi(a|s)/Z(s)$, with the normalization factor $Z(s) = \int_a \frac{\beta}{\text{Var}[Q(s, a)]} \pi(a|s)$ as in equation 3. Assume that 1) $\forall s : Z(s) \geq 1$ and 2) Q is bounded ($\forall s, a : |Q(s, a)| \leq Q_m$).*

Then for any $C \in \mathbb{R}$, there exists β, K such that

$$P \left(\max_{\pi'} \mathbb{E}_{\pi'} [\delta(s, a)] \geq C \right) \leq \frac{1}{K^2}$$

Proof. We firstly apply triangle inequality to unwrap the original formulation into a sum of two differences, and bound the two terms respectively.

$$\begin{aligned} & \max_{\pi'} \mathbb{E}_{\pi'} [\delta(s, a)] \\ &= \max_{\pi'} \mathbb{E}_{\pi'} \left[\sup_k |Q_k(s, a) - \mathcal{T}^\Pi Q_{k-1}(s, a)| \right] \\ &= \max_{\pi'} \mathbb{E}_{\pi'} \left[\sup_k |Q_k(s, a) + E[Q_k(s, a)] \right. \\ & \quad \left. - E[Q_k(s, a)] - \mathcal{T}^\Pi Q_{k-1}(s, a)| \right] \\ & \leq \max_{\pi'} \mathbb{E}_{\pi'} \left[\sup_k |Q_k(s, a) - E[Q_k(s, a)]| \right] + \\ & \quad \max_{\pi'} \mathbb{E}_{\pi'} \left[\sup_k |E[Q_k(s, a)] - \mathcal{T}^\Pi Q_{k-1}(s, a)| \right] \end{aligned}$$

Starting with the red term, we firstly obtain a probabilistic bound on the distance term inside the expectation with the Chebyshev's inequality

$$P(|X - E[X]| \geq \sigma K) \leq \frac{1}{K^2}$$

$$\begin{aligned} & P \left(|Q_k(s, a) - E[Q_k(s, a)]| \geq K \sqrt{\text{Var}[Q_k(s, a)]} \right) \leq \frac{1}{K^2} \\ & P \left(\frac{\beta}{\sup_k \sqrt{\text{Var}[Q_k(s, a)]}} |Q_k(s, a) - E[Q_k(s, a)]| \geq \beta K \right) \leq \frac{1}{K^2} \end{aligned}$$

Secondly, note that by assumption $|Q|$ is bounded by Q_m . This provides us an upper-bound on the difference $|Q(s, a) - E[Q(s, a)]| \leq 2Q_m$. Making use of both the

general upper-bound and the tight probabilistic bound, by setting $\pi'(a|s) = \frac{\beta}{\sup_k \sqrt{\text{Var}[Q_k(s,a)]}} \pi(a|s)/Z(s)$, we have

$$\begin{aligned} & \max_{\pi'} \mathbb{E}_{\pi'} \left[\sup_k |Q_k(s,a) - E[Q_k(s,a)]| \right] \\ &= \max_{\pi'} \mathbb{E}_{\pi} \left[\frac{\beta}{\sup_k \sqrt{\text{Var}[Q_k(s,a)]}} \sup_k |Q_k(s,a) - E[Q_k(s,a)]| / Z(s) \right] \\ &\leq \left(1 - \frac{1}{K^2}\right) \beta K + \frac{2}{K^2} Q_m \leq B \end{aligned}$$

By assumption $Z(s) \geq 1$ and can be safely ignored. By picking the appropriate K and β , we can bound the **red** term by any constant $B \in \mathbb{R}$. The same bound holds for the **blue** term since $E[\mathcal{T}^\Pi Q_{k-1}(s,a)] = E[Q_k(s,a)]$. We therefore arrive at a constant bound for the Bellman error term $\max_{\pi'} \mathbb{E}_{\pi'} [\delta(s,a)]$. \square

Note that in Theorem A.2 Assumption 1) does not change the optimization problem in equation 4, 5 and Assumption 2) can be easily satisfied by imposing Spectral Norm on the Q function.

Now according to the constant bound on $\delta(s,a)$ from Theorem A.2, the convergence of our proposed framework follows directly from Theorem A.1 (Kumar et al., 2019; Farahmand et al., 2010; Munos, 2003), with the set of policies $\Pi' = \left\{ \pi' \mid \pi'(a|s) = \frac{\beta}{\sup_k \sqrt{\text{Var}[Q_k(s,a)]}} \pi(a|s)/Z(s), \pi \in \Pi \right\}$.

A.2. Training Time of MC Dropout

Since the most time is spent during training is at communication between the GPU and CPU when performing roll-outs for evaluation. UWAC with dropout takes less than 1.5 times the training time of BEAR, with 100 times the original batchsize calculating sample uncertainty (in parallel on a single GPU).

A.3. Observations on the Q Value Divergence of BEAR

We tested BEAR learning rate from $\{10^{-3}, 10^{-4}, 10^{-5}\}$, the divergence behavior did not change. The action support constraint of BEAR is helpful, but it relies on the MMD approximation which is not perfect. Intuitively, UWAC provides a complementary enforcement to the action support constraint, where OOD actions that survive the MMD loss are further penalized.

B. Figures

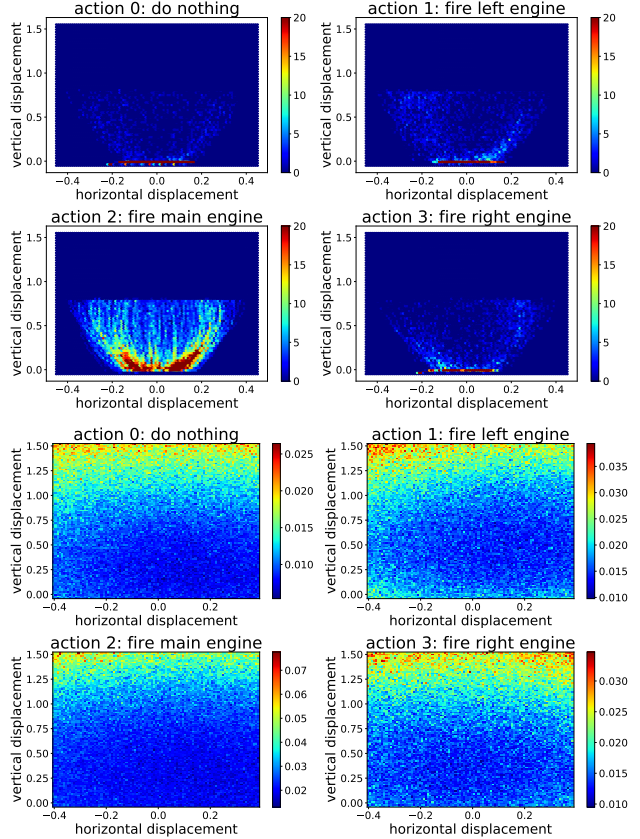


Figure 7: **Top.** The training dataset has observations with vertical displacements > 0.8 removed. This makes all states on the top OOD states. **Bottom.** Our model estimates higher uncertainty (brighter color) on the top and lower uncertainty (colder color) on the bottom.

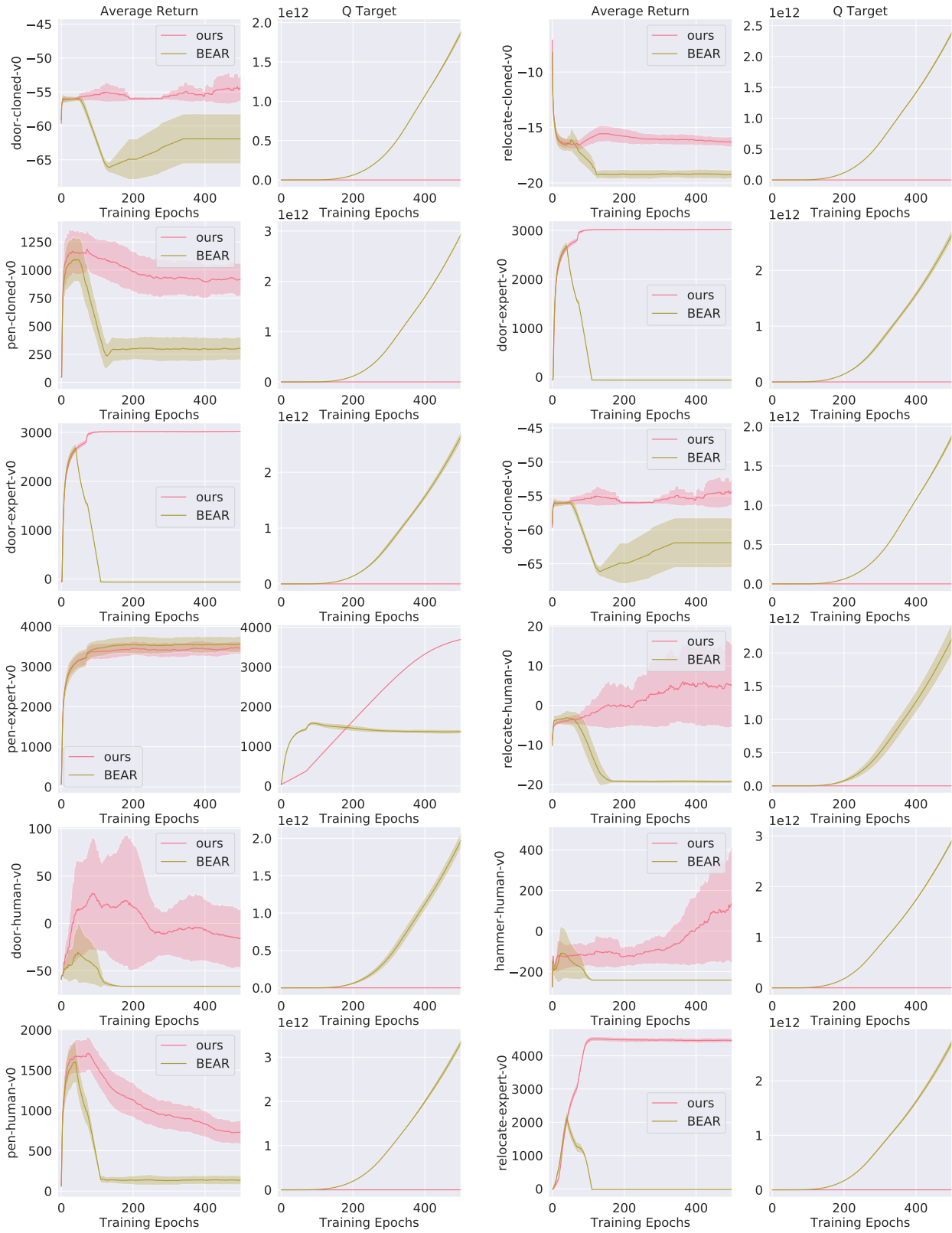


Figure 8: Plot of average return v.s. training epochs, together with the corresponding average Q Target over training epochs on the D4RL Adroit hand offline data set. Results are averaged across 5 random seeds. Note that the performance of baseline (BEAR) degrades over time (also noted in original paper (Kumar et al., 2019)), and the Target Q value explodes. Our method, UWAC, achieves significantly better overall performance and training stability.

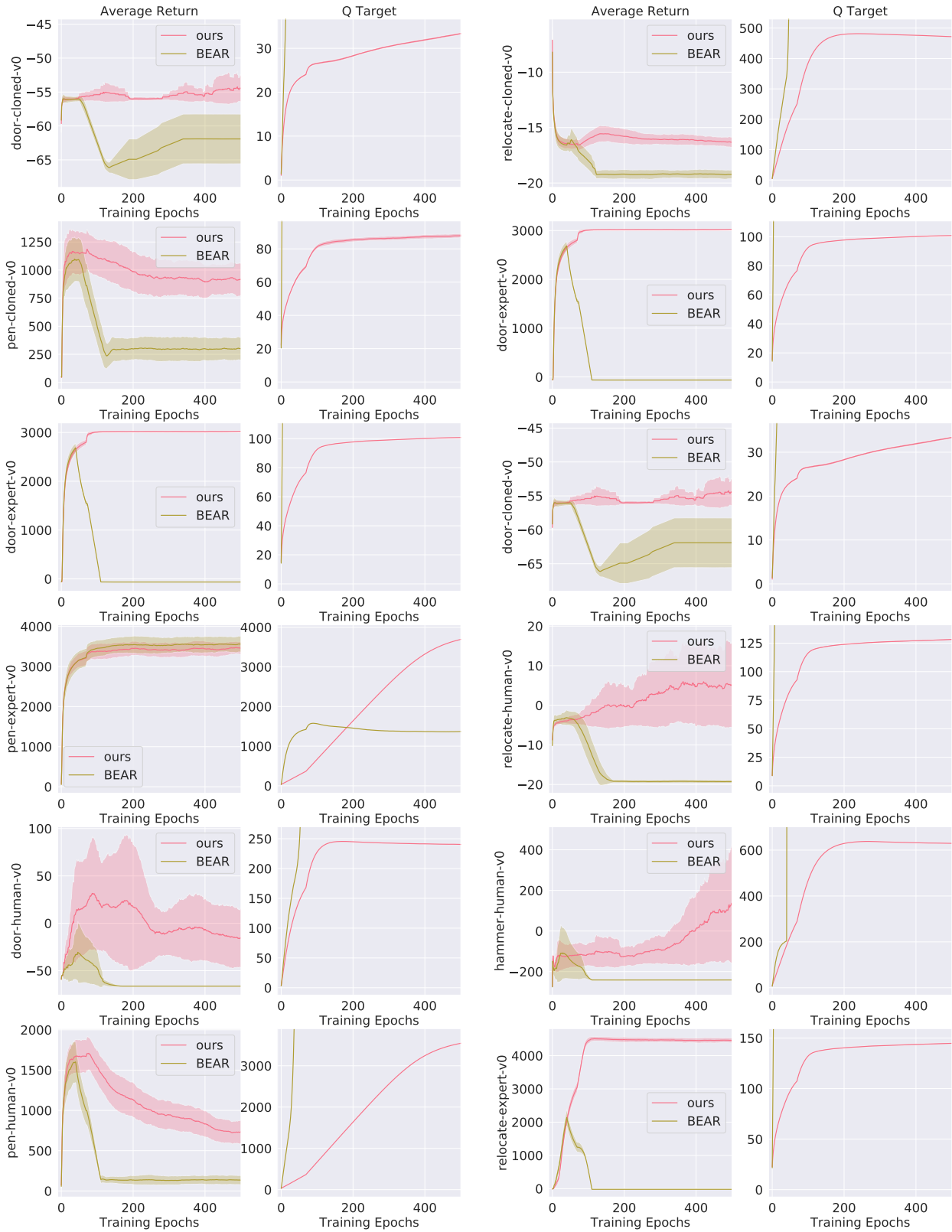


Figure 9: Plot of average return v.s. training epochs (zoomed-in). The figure is the same as 8, except that the second column is zoomed-in on the Q values of the UWAC critic.

Uncertainty Weighted Actor-Critic for Offline Reinforcement Learning

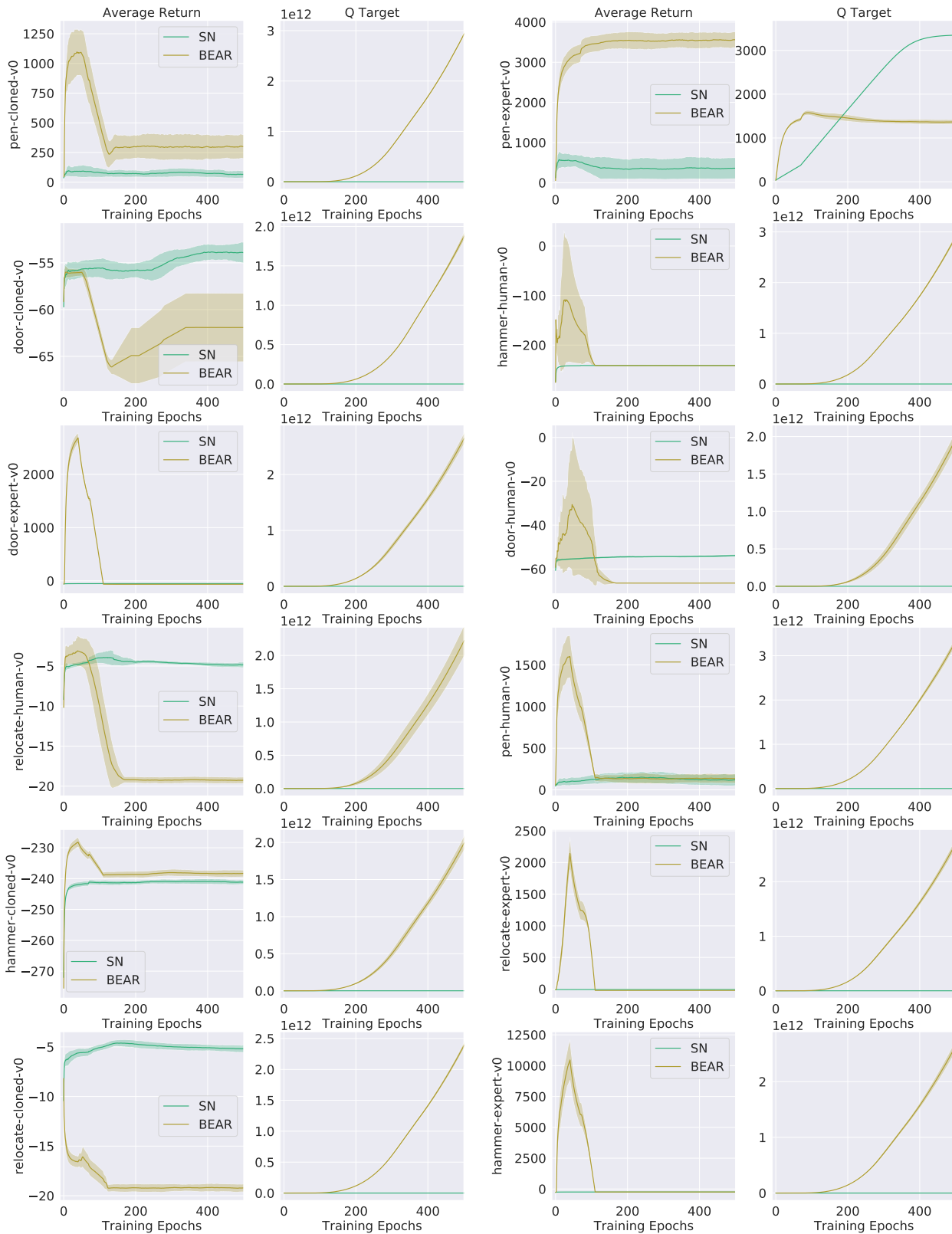


Figure 10: **Ablation:** Plot of average return v.s. training epochs for BEAR v.s. BEAR+Spectral Norm, together with the corresponding average Q Target over training epochs on the D4RL Adroit hand offline data set. Results are averaged across 5 random seeds. Although BEAR with Spectral Normalized Q function maintains stable Q estimate during training, BEAR with SN often achieves significantly worse training performance in terms of average return.

Uncertainty Weighted Actor-Critic for Offline Reinforcement Learning

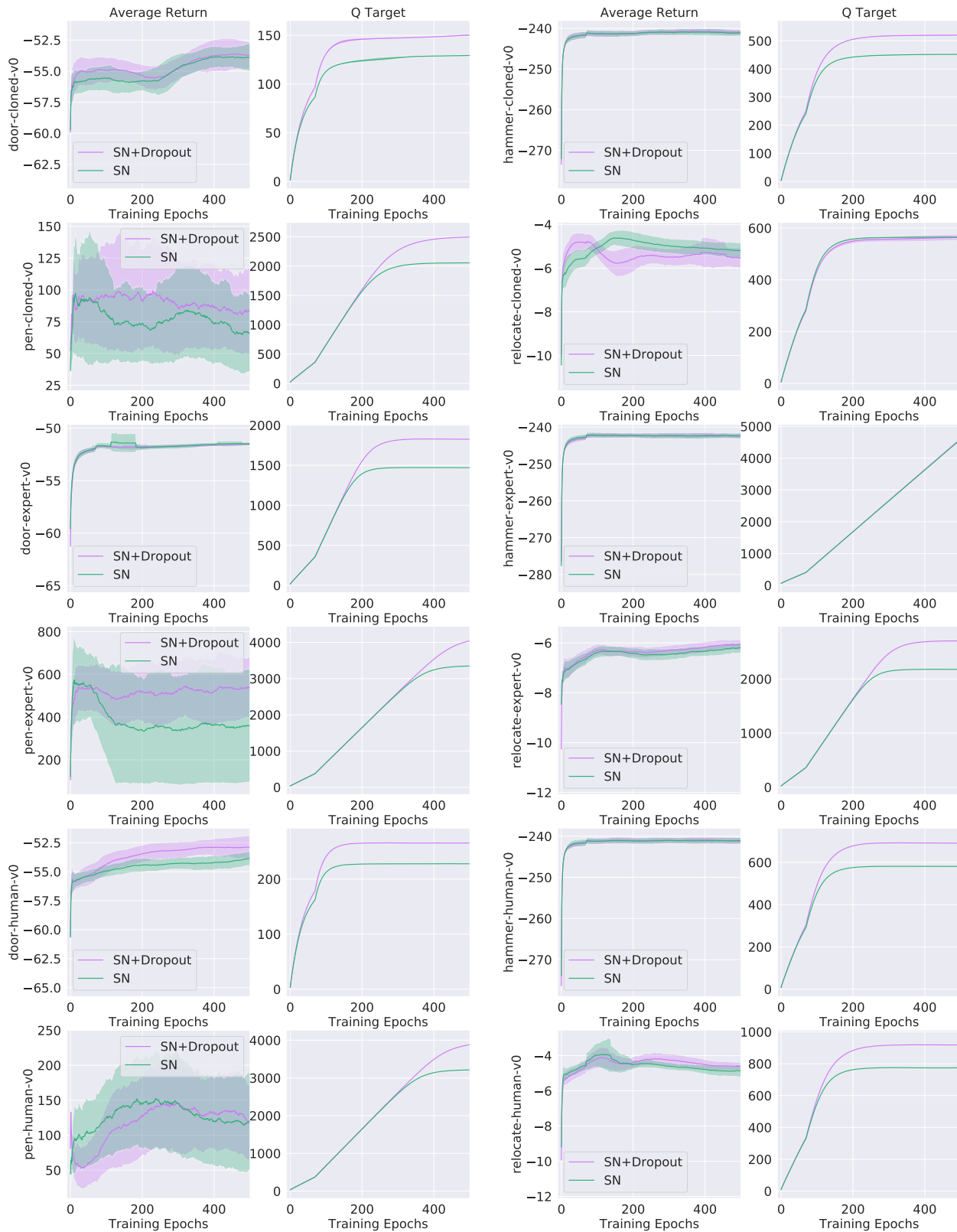


Figure 11: **Ablation:** Plot of average return v.s. training epochs for BEAR+Spectral Norm v.s. BEAR+Dropout+Spectral Norm, together with the corresponding average Q Target over training epochs on the D4RL Adroit hand offline data set. The results are averaged across 5 random seeds. Without the UWAC reweighing loss, performing dropout on the Q function does not lead to improved performance.

Uncertainty Weighted Actor-Critic for Offline Reinforcement Learning

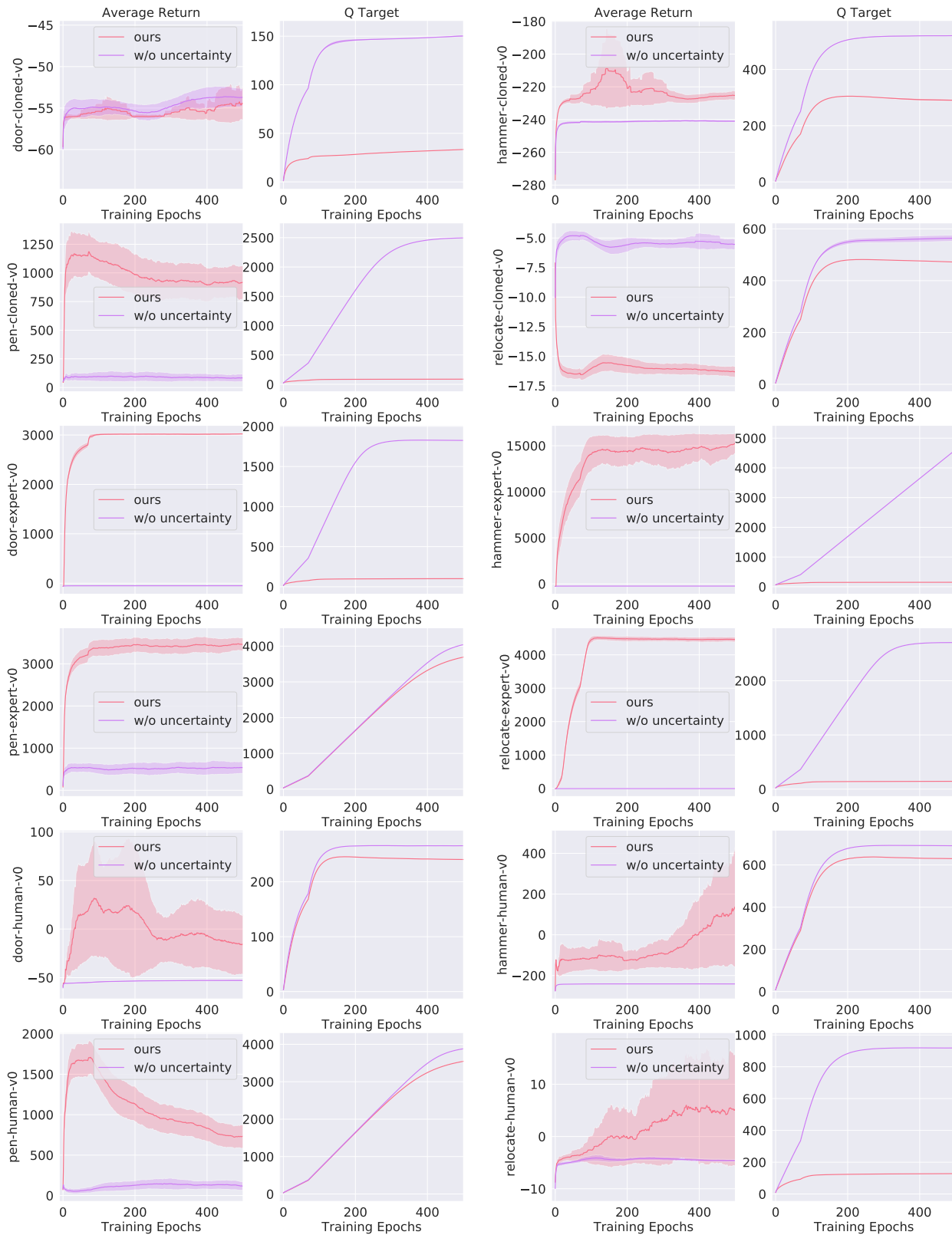


Figure 12: **Ablation:** Plot of average return v.s. training epochs for UWAC (ours) v.s. ours without uncertainty weighing but with dropout in the Q function, together with the corresponding average Q Target over training epochs on the D4RL Adroit hand offline data set. The results are averaged across 5 random seeds. Without the weighing loss, performance of the agent drops drastically. Note that low performance on hammer-cloned, door-cloned, and relocated-cloned may be attributed to the bad quality of the datasets caused by data collection (explained in section 5.3)

Uncertainty Weighted Actor-Critic for Offline Reinforcement Learning

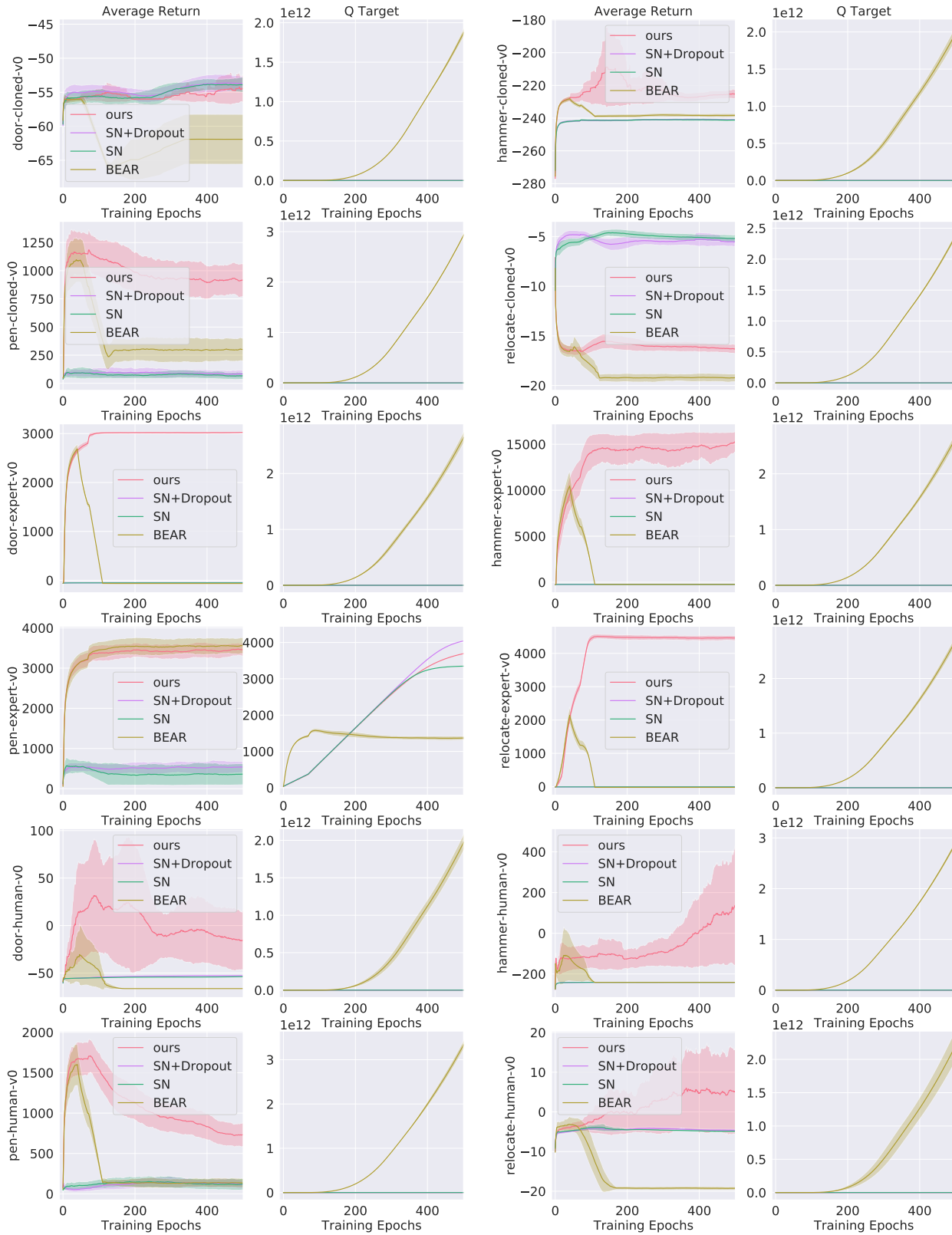


Figure 13: **Ablation:** Figure 10, 11, 12 plotted together. Note that SN+Dropout (purple) is also denoted as ours-w/o-uncertainty in Figure 12.

Uncertainty Weighted Actor-Critic for Offline Reinforcement Learning

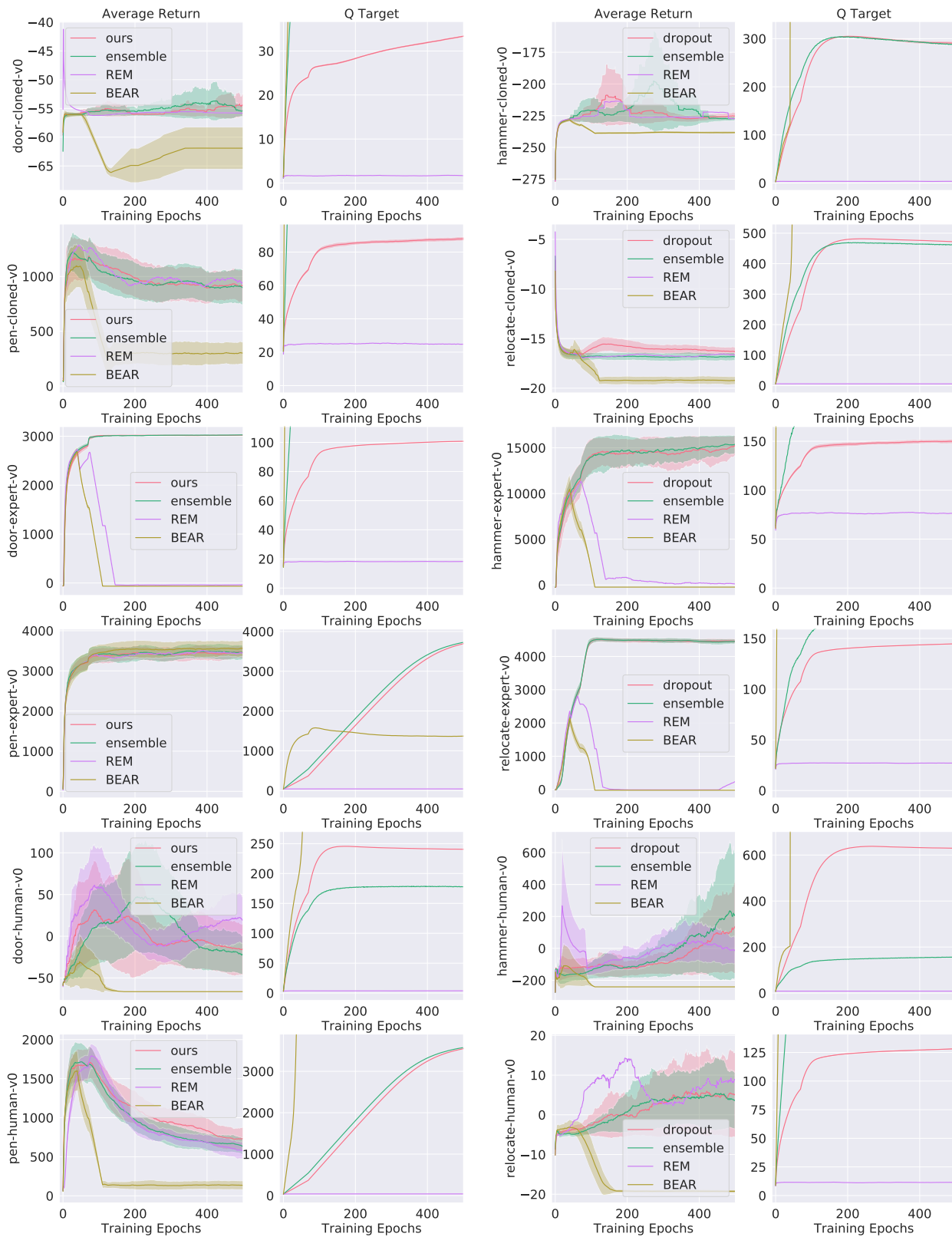


Figure 14: **Ablation:** Plot of UWAC under dropout (ours), Averaged-DQN ensembles, REM against baseline BEAR.

Uncertainty Weighted Actor-Critic for Offline Reinforcement Learning

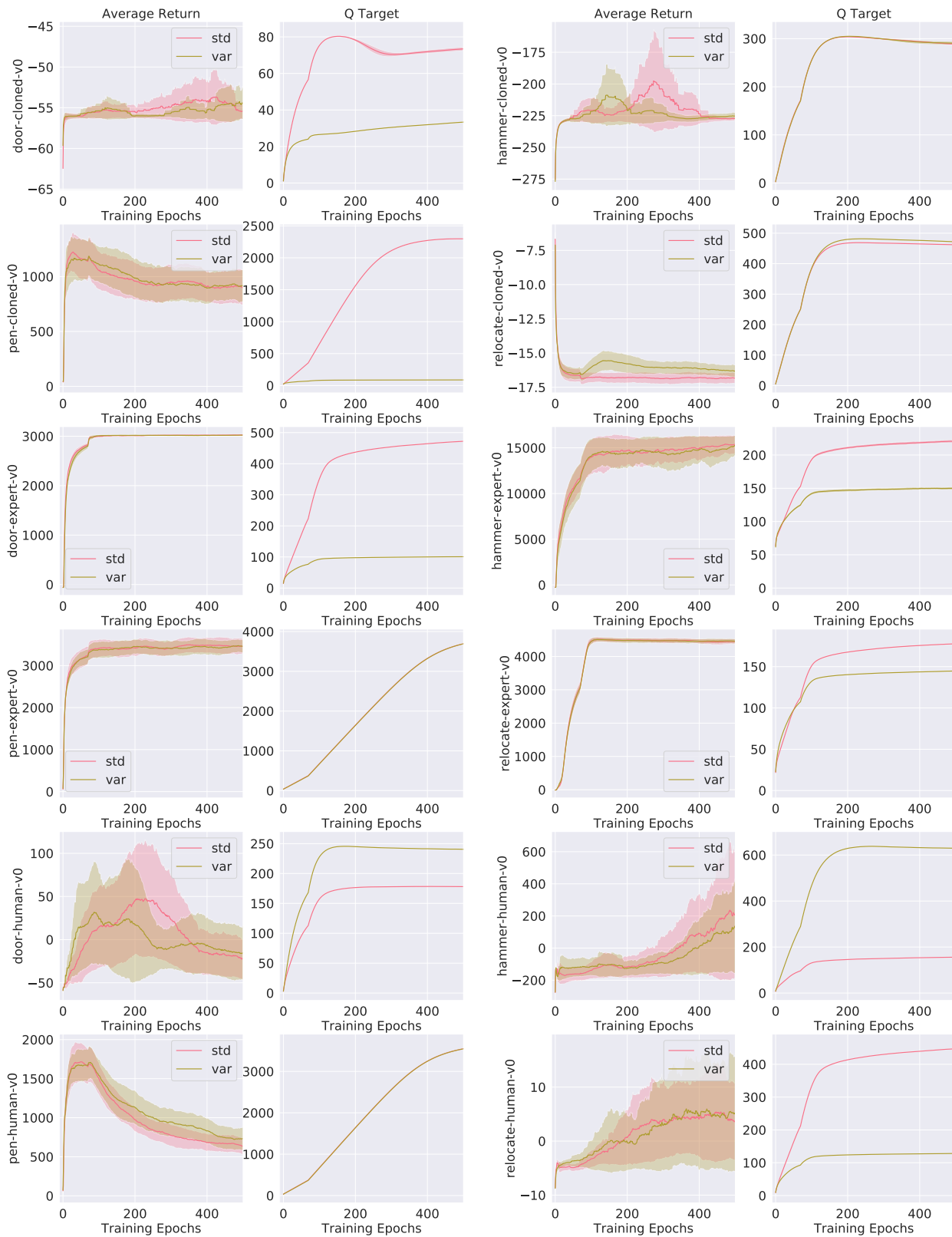


Figure 15: **Ablation:** Plot of UWAC with variance down-weighting v.s. standard deviation down-weighting.

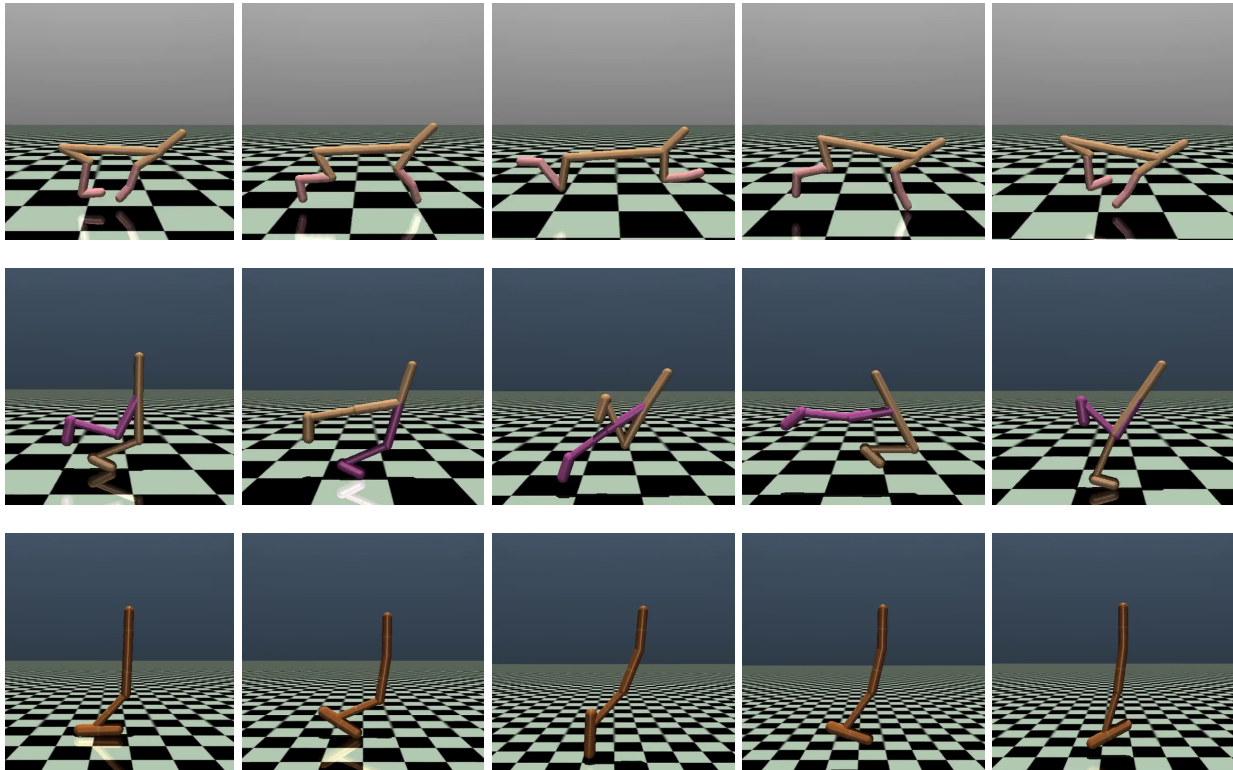


Figure 16: Sequences of our offline agent trained from expert demonstrations executing learned policies performing on the halfcheetah, walker2d, and hopper tasks in the MuJuCo Gym environment. See the videos attached in the supplementary.

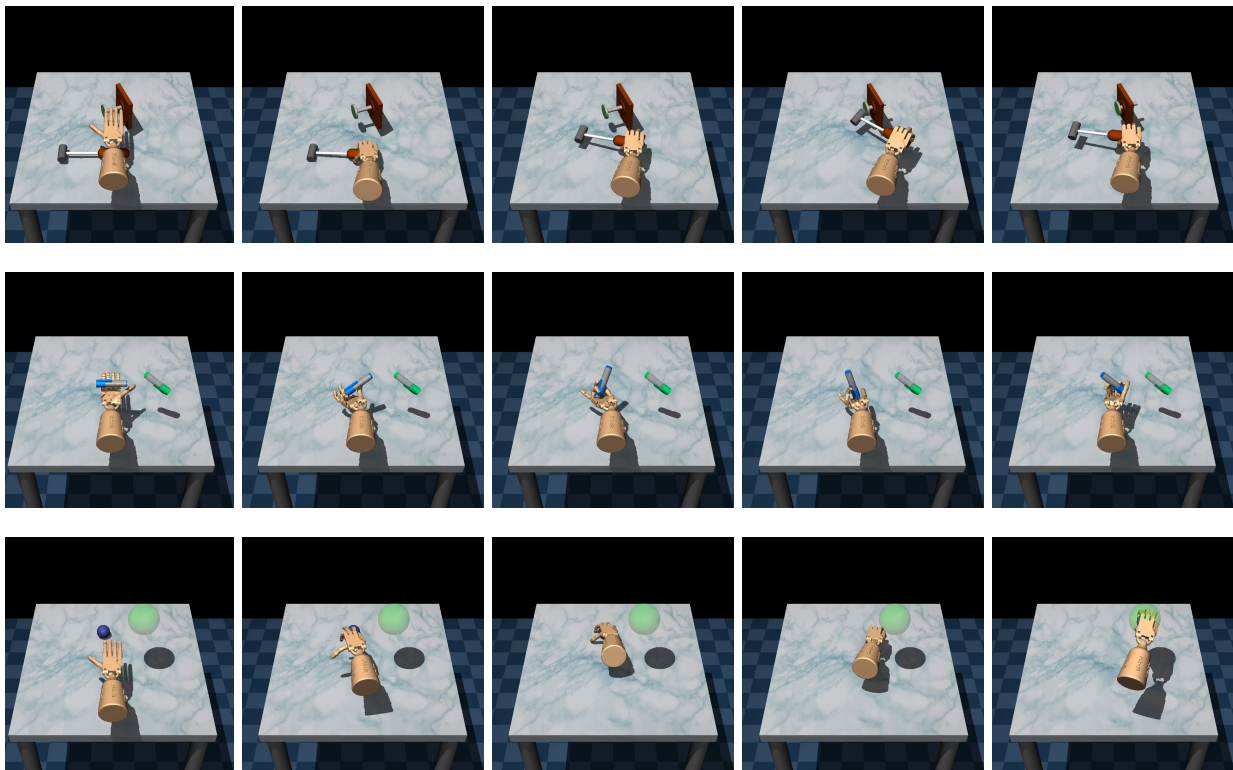


Figure 17: Sequences of the agent trained from human demonstrations executing learned policies performing the Adroit tasks of hammering a nail, twirling a pen and picking/moving a ball. The task of opening a door is shown in Figure 5. See the videos attached in the supplementary.